Redox Biology 29 (2020) 101407

Contents lists available at ScienceDirect

Redox Biology

journal homepage: www.elsevier.com/locate/redox

Neuronal vulnerability to fetal hypoxia-reoxygenation injury and motor deficit development relies on regional brain tetrahydrobiopterin levels

Jeannette Vasquez-Vivar[a,1], Zhongjie Shi[b,1], Jeong-Won Jeong[b,c], Kehuan Luo[b], Amit Sharma[d], Karthikeyan Thirugnanam[a], Sidhartha Tan[b,d,*]

[a] Department of Biophysics and Redox Biology Program, Medical College of Wisconsin, Milwaukee, WI, USA
[b] Department of Pediatrics, Wayne State University School of Medicine, Detroit, MI, USA
[c] Department of Neurology, Wayne State University School of Medicine, Detroit, MI, USA
[d] Neonatology Division, Children's Hospital of Michigan, Detroit, MI, USA

ARTICLE INFO

Keywords:
Infant newborn
Cerebral palsy
Hypertonia
Sepiapterin
Free radicals
Fetal brain

ABSTRACT

Hypertonia is pathognomonic of cerebral palsy (CP), often caused by brain injury before birth. To understand the early driving events of hypertonia, we utilized magnetic resonance imaging (MRI) assessment of early critical brain injury in rabbit fetuses (79% term) that will predict hypertonia after birth following antenatal hypoxia-ischemia. We examined if individual variations in the tetrahydrobiopterin cofactor in the parts of the brain controlling motor function could indicate a role in specific damage to motor regions and disruption of circuit integration as an underlying mechanism for acquiring motor disorders, which has not been considered before. The rabbit model mimicked acute placental insufficiency and used uterine ischemia at a premature gestation. MRI during the time of hypoxia-ischemia was used to differentiate which individual fetal brains would become hypertonic. Four brain regions collected immediately after hypoxia-ischemia or 48 h later were analyzed in a blinded fashion. Age-matched sham-operated animals were used as controls. Changes in the reactive nitrogen species and gene expression of the tetrahydrobiopterin biosynthetic enzymes in brain regions were also studied. We found that a combination of low tetrahydrobiopterin content in the cortex, basal ganglia, cerebellum, and thalamus brain regions, but not a unique low threshold of tetrahydrobiopterin, contributed etiologically to hypertonia. The biggest contribution was from the thalamus. Evidence for increased reactive nitrogen species was found in the cortex. By 48 h, tetrahydrobiopterin and gene expression levels in the different parts of the brain were not different between MRI stratified hypertonia and non-hypertonia groups. Sepiapterin treatment given to pregnant dams immediately after hypoxia-ischemia ameliorated hypertonia and death. We conclude that a developmental tetrahydrobiopterin variation is necessary with fetal hypoxia-ischemia and is critical for disrupting normal motor circuits that develop into hypertonia. The possible mechanistic pathway involves reactive nitrogen species.

1. Introduction

Perinatal hypoxia-ischemia (H–I) is etiologically linked to childhood motor disorders. Cerebral palsy (CP) is the most common movement disorder in children. The definitive diagnosis of motor deficits of CP is made not at birth but at approximately 18–24 months of age. Hypertonia is a pathognomonic feature of CP. We have established a fetal H–I rabbit model of CP that, unlike other H–I animal models, manifests newborn hypertonia and postural changes mimicking the human condition [1]. Another advantage of this model is that intrinsic etiologies can be investigated by comparing fetuses that are not affected with those that develop hypertonia in the same litter.

Since neurobehavioral deficits in the animal model are only evident months after birth but the etiological injury could be before birth, at the time of brain H–I and reperfusion, we needed to have a marker that discerns affected from non-affected fetuses. For this purpose, we developed a magnetic resonance imaging (MRI) biomarker during H–I that identifies fetuses that will develop newborn hypertonia [2,3]. Brain corticospinal tract integrity can be evaluated using a measure of random water diffusion in a period of time using MRI with diffusion-weighted imaging (DWI). The impedance of water diffusion in tissue is quantified by apparent diffusion coefficient (ADC) in a specific region

* Corresponding author. Department of Pediatrics, Children's Hospital of Michigan, 3901 Beaubien Street, Detroit, MI, 48201, USA.
E-mail address: sidhartha.tan@wayne.edu (S. Tan).
[1] First two authors contributed equally to the manuscript.

https://doi.org/10.1016/j.redox.2019.101407
Received 1 October 2019; Received in revised form 13 November 2019; Accepted 9 December 2019
Available online 12 December 2019

of interest and is used as a measure of brain integrity. In monitoring ADC obtained during rabbit fetal H–I at 79% gestation, two patterns of ADC predicted hypertonia in the newborn [2,3]. One of the two patterns reflected reperfusion-reoxygenation injury that was caused by elevated levels of superoxide radical anion production [3]. Thus, the MRI biomarker allowed us to investigate predisposing and downstream factors at multiple time points that would explain the increased risk of developing hypertonia.

The motor pathway determining hypertonia involve varied brain regions located in multiple interconnected cortical and subcortical structures. Disruption in the communication of motor-related brain regions from neuronal dysfunction, neurotransmitter deficiency and/or injury to white matter tracts will result in motor deficits. Tetrahydrobiopterin is a cofactor of several important enzymes that regulate neurometabolism by regulating production of monoamine neurotransmitters [4,5] and nitric oxide [6,7]. Moreover, tetrahydrobiopterin plays a key role regulating cellular redox signaling by inhibiting nitric oxide synthase (NOS) uncoupling. Movement disorder is characteristic of congenital deficiencies in tetrahydrobiopterin due to mutations in the enzymes of the synthetic and recycling pathways causing a decrease of dopamine and serotonin signaling in the brain. Tetrahydrobiopterin deficiency is diagnosed by sampling spinal fluid and genetic testing. These assays, however, report global but not brain region-specific variations, and, as such, it is impossible to establish the significance of tetrahydrobiopterin changes in motor-pathways and its mechanisms.

Previously we showed that cumulative increases of tetrahydrobiopterin in the thalamus, basal ganglia, and cortex occur in naïve fetal brains between 70%–92% gestation, suggesting a role in normal development [8]. In a study to examine if tetrahydrobiopterin influenced neuronal survival, neuronal cultures from different brain regions of basal ganglia, cortex, and thalamus at 70% and 92% gestation, we showed differential regional susceptibility to *ex vivo* tetrahydrobiopterin levels, especially following H–I, with the thalamus being most vulnerable in the preterm age [9]. Increasing tetrahydrobiopterin, however, improved neuronal survival after H–I especially in the premature thalamus [9].

Previously, we hypothesized that low tetrahydrobiopterin levels normally found in prematurity would fall below a threshold of injury during antenatal H–I to cause brain injury [10]. The possibility that regional tetrahydrobiopterin concentration is the critical factor determining outcomes of “low” tetrahydrobiopterin has not been addressed. Herein, we tested the hypothesis that endogenous tetrahydrobiopterin level before H–I in selected brain regions is responsible for either susceptibility or resistance to H–I injury and motor deficits. Our secondary hypothesis was that low tetrahydrobiopterin along with H–I-reperfusion injury determines the pathogenic mechanism of hypertonia, involving reactive species. Also, we examined if individual variations in the tetrahydrobiopterin cofactor in different parts of the brain could indicate a role in specific damage in motor neurons and disrupted circuit integration as an underlying mechanism for acquiring motor disorders. We reasoned that investigating fetuses exhibiting MRI patterns predictive of hypertonia would better elucidate a role for regional susceptibilities. Our data indicate that H–I-induced hypertonia is determined by a regional combinatorial effect of low tetrahydrobiopterin rather than a one-region low threshold after antenatal H–I. Our data also indicate that a tetrahydrobiopterin analog, sepiapterin, may be a potential neuroprotectant even administered after the antenatal insult.

2. Materials and methods

The Institutional Animal Care and Use Committee of Wayne State University (Detroit, MI) approved all experimental procedures with animals.

2.1. Surgery and imaging

The surgical procedure previously was described in detail [3]. Briefly, pregnant New Zealand white rabbit dams at 25 days gestation (E25) or 79% gestation (the term being 31.5 days) were anesthetized with an initial regimen of intravenous fentanyl (75 μg/kg/h) and droperidol (3.75 mg/kg/h) followed by epidural anesthesia using 0.75% bupivacaine with continuous infusion of about one-third lower initial intravenous anesthetic dose. A balloon catheter was introduced into the left femoral artery and advanced into the descending aorta to above the uterine arteries and below the renal arteries. The catheterized animal was placed inside an MRI scanner. Body core temperature was monitored with a rectal temperature probe and maintained at 37 ± 0.3 °C with a water blanket wrapped around the dam's abdomen and connected to a temperature-controlled heating pump. Acquisition of fetal MRI began after the dam was positioned in the magnet. After a baseline period, the aortic balloon was inflated for 40 min. Inflating the balloon causes uterine ischemia and subsequent global fetal hypoxia and H–I in fetal brains. At the end of H–I, the balloon was deflated, which started the reperfusion period. Acquisition of MRI was continued 20 min after the end of uterine ischemia to capture the changes during uterine reperfusion. After the imaging session, the dams were either immediately C-sectioned for delivery of fetuses (immediate group, 0 h), or the catheter was removed, the femoral artery was repaired, and the dam was allowed to recover. Two days after H–I, at E27, all fetuses were delivered by C-section (48 h group). The rabbit pregnant dams that underwent sham surgery did not have MRI. In these dams the femoral artery was isolated, the balloon catheter was introduced similar to the procedure for H–I animals but the balloon was not inflated. The dams were immediately C-sectioned for delivery of fetuses (immediate group, 0 h) or the femoral artery was repaired after removal of the catheter and the dam was allowed to recover after surgery. Fetuses were delivered by C-section after two days (E27, 48 h group).

2.2. MRI with diffusion-weighted imaging

Dams were imaged serially *in utero* on a Siemens MAGNETOM Verio 3T MR scanner with an eight-channel knee coil (Siemens Medical Solution, Erlangen, Germany). High-resolution single-shot turbo-spin echo T2-weighted three plane images (HASTE, TR/TE = 1500/80 ms, slice thickness = 4 mm, matrix = 256 × 157, field of view = 256 mm with 30–45 axial slices covering all fetuses inside dam) were acquired in axial, coronal, and sagittal planes to identify the sequential position of each fetus in uterine horns. Additional turbo-spin-echo T2-weighted images (TSE, TR/TE = 6100/95 ms) were taken for anatomical reference in the axial plane, with 25–32 axial slices covering all fetal brains. Slice thickness was 4 mm with matrix = 256 × 192 and field of view = 160 mm. Single-shot echo-planar imaging diffusion-weighted sequence with b = 0 and 800 s/mm^2, TR/TE = 6600/100 ms, and NEX = 1 were acquired with the same geometry and resolution as the anatomical reference scan.

2.3. MRI data analysis

The position of each fetus in each uterine horn and corresponding fetal brain was identified using 3D cross-sectional single-shot datasets in eFilm workstation 4.2 (Merge Healthcare, Chicago, IL). ADC maps of each identified fetal brain defined by a polygon region of interest to cover the whole brain in three orthogonal planes were calculated off-line using in-house software written in Matlab (MathWorks, Natick, MA). Only those fetuses that survived had the MRI analyzed.

Four patterns of fetal MRI changes occurred with uterine ischemia: Pattern I had no change in ADC throughout, Pattern II showed a fall in ADC but not below 85% of the baseline ADC value, Pattern III showed a fall in ADC below 85% of the baseline ADC value and had immediate recovery of ADC with uterine reperfusion, and Pattern IV showed a

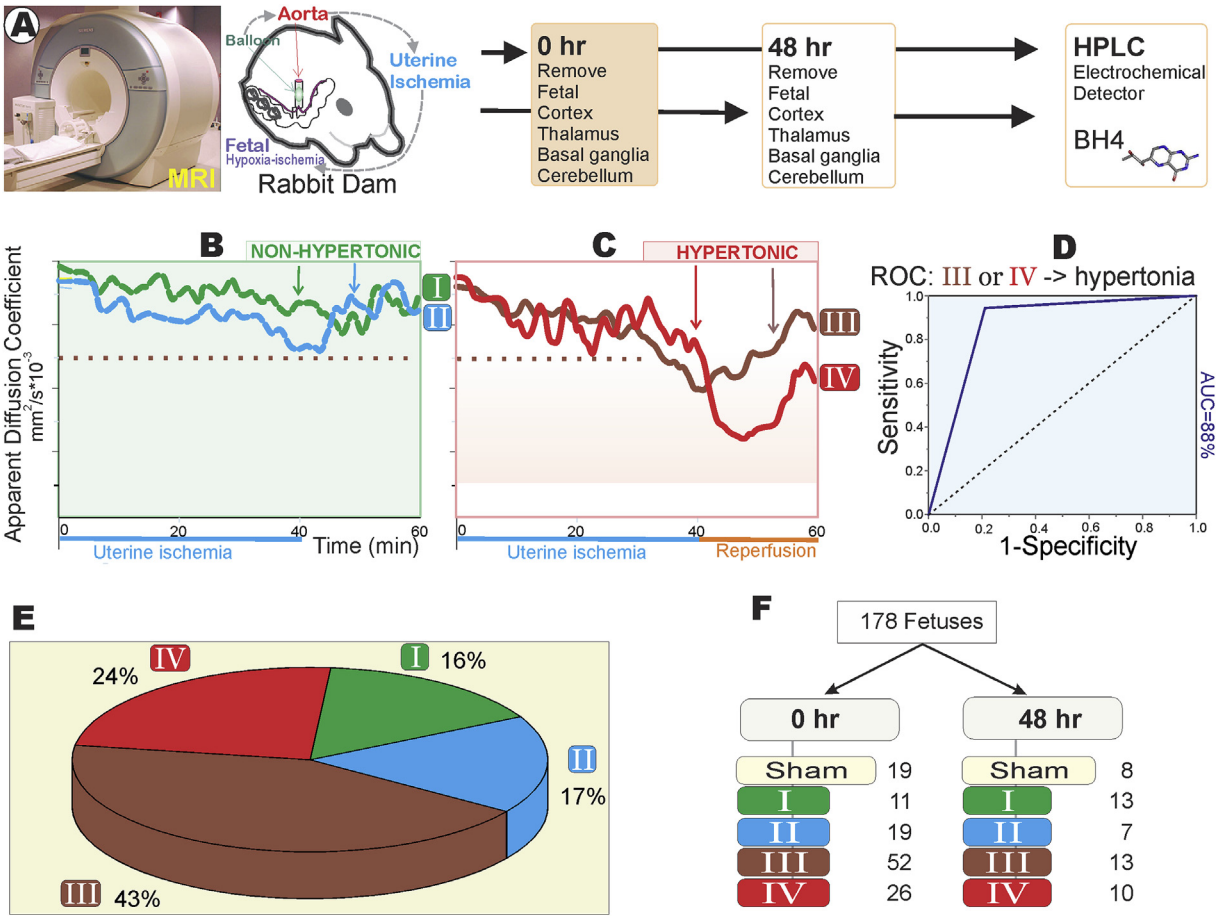

Fig. 1. Fetal brain H–I protocol and MRI predictive biomarker. (A) Pregnant rabbit dam at E25 underwent MRI before, during, and after uterine ischemia. After imaging fetal brain tissue collected 20 min after (0 h) or after 48 h following uterine ischemia (48 h). Fetal brains regions assayed for BH4. **(B)** Patterns of ADC change (ordinate) in fetal brain. Pattern I (green) shows no significant change from baseline. Pattern II (blue) shows a drop from baseline during H–I but not below a threshold (dotted brown line). **(C)** Pattern III (brown) shows a drop from baseline below the threshold. Pattern IV (red) shows a further drop after the end of H–I during uterine reperfusion. **(D)** Patterns III or IV are predictive of hypertonia found postnatally. The receiver operating characteristic curve shows area under curve of 88%. **(E)** The subpopulations of MRI patterns as a percentage of all surviving fetuses undergoing H–I. **(F)** Number of fetuses stratified according to time of tissue collection and their MRI pattern. There were no deaths at 0 h and 7 deaths at 48 h. MRI was not analyzed for the dead fetuses. (For interpretation of the references to color in this figure legend, the reader is referred to the Web version of this article.)

further fall in ADC after the end of uterine ischemia and during uterine reperfusion with eventual recovery (Fig. 1B and C). If fetal deaths occurred, the MRI patterns were not analyzed further. Patterns III and IV have been shown to predict hypertonia in the newborn period [3] while the first two patterns predict normal or mild motor deficits. Classification of all results was done with an MRI predictive biomarker of Hypertonia (pattern III or IV) and compared with that of Non-hypertonia (pattern I or II).

MRI was used as a surrogate to determine which fetuses became hypertonic, since we sacrificed fetuses at two time points (0 h and 48 h) after H–I.

2.4. Biochemical assays

Tetrahydrobiopterin analysis in parts of the brains: A single-blind randomized protocol was implemented. Sample identifiers other than the brain region were blinded until the end of the high-performance liquid chromatography analysis. In both groups, after C-section, fetal brains were extirpated and four brain regions—the cortex, basal ganglia, thalamus, and cerebellum—were isolated. The genders of the fetuses were determined.

Tissues were immediately frozen in liquid nitrogen. Frozen tissues were thawed and homogenized in a 50 mM cold phosphate buffer, pH 2.6. Samples were deproteinized by filtration using a pre-washed Amicon filter membrane with 10 KDa cutoff. It was estimated previously that more than 95% of tetrahydrobiopterin was recovered after filtration, while protein was decreased by more than 80%. Clean supernatants were loaded onto a Synergi-Hydro RP column (250 × 4.6 mm, Phenomenex, CA), and tetrahydrobiopterin was analyzed by electrochemical detection using four-electrode cells with applied potential set at 0, 150, 260, and 365 mV. Concentrations were calculated using normalization of authentic standards, and protein content was measured by bicinchoninic acid assay in each sample.

Tetrahydrobiopterin enzyme cloning and qRT-PCR analysis: First, rabbit genes for the enzymes involved in tetrahydrobiopterin production and recycling were identified; then they were cloned using RACE-based techniques (SMARTer RACE 5′/3′ Kit, Clontech Laboratories) by lab-designed gene-specific primers for rabbit sequences through Primer-Blast (http://www.ncbi.nlm.nih.gov/tools/primer-blast). cDNA sequencing was performed using a 96-capillary automated DNA sequencer (Applied Biosystems 3730XL) and confirmed by alignment with the predicted sequences at GenBank. The rabbit gene sequence and GenBank ID has recently been published [11].

Total RNA was purified from the cortex, cerebellum, and thalamus using the PureLink RNA Mini Kit (Life Technologies, Grand Island, NY) as done previously [11]. Samples were chosen in pairs of either high or low tetrahydrobiopterin levels. The High-Capacity RNA-to-DNA Kit (Applied Biosystems, Foster City, CA) was used for reverse

Table 1
RT-PCR primers.

Gene	Forward (5′-3′)	Reverse (5′-3′)
GTPCH	AGTTGGGGTGGTGGTTGAAG	TCTTCCCGAGTCTTGGGGTC
PTPS	CCGTTACGGGAATGGTTATGA	TGAAGTACGGCACATCCAGG
SPR	TGAACATCTCGTCGCTGTGT	AGCTTCTGGGCTGACTCCTT
DHPR	TTGGATGGGACTCCTGGGAT	GTATCCAGGGTAACCGGCAG
DHFR	caCAACGTCGTCAGTGGAAGG	ccTTGTGGCGGTTCCTTGAG

transcription. The RT-PCR was performed in a StepOnePlus real-time PCR System (Applied Biosystems) using the 2x SYBR Green qPCR Master Mix (Biotool.com). Reactions were performed in duplicates in MicroAmp optical 96-well plates (ThermoFisher Scientific, Waltham, MA) with a total volume of 10 μL comprising the final concentration of 1x SYBR Green PCR Master mix, cDNA (10 ng), and primers (75 nM; forward and reverse primers listed in Table 1).

The following thermal protocol was used: initial incubation at 95 °C for 10 min, 40 cycles of 15 s at 95 °C, and 1 min at 60 °C. The cycle threshold values of individual genes were subtracted from the cycle threshold values for hypoxanthine phosphoribosyltransferase 1 (HPRT1, a hypoxia-stable housekeeping gene), and were then used to calculate the fold change in relative gene expression (2–ΔΔCT). The results were compared with the MRI pattern I group (*i.e.*, no change in ADC).

2.5. Nitrotyrosine detection

Nitrotyrosine is a biomarker of reactive nitrogen species produced under conditions of oxidant injury. Nitrotyrosine in different parts of the brain was analyzed using an immunoassay performed by an automated Western blot system (WES, Protein Simple, CA). Tissue samples were probed with a primary antibody to nitrotyrosine (Abcam, ab7048), a negative primary antibody control, and another negative control with antibody pretreated with nitrated bovine serum albumin which is important for differentiating specific from nonspecific binding of the antibody. The nitrated protein chromatograms was analyzed for the difference between the areas of the peaks resolved between 12 to 180 KDa between the primary-antibody chromatogram and pretreated-antibody chromatogram.

2.6. Sepiapterin treatment

Sepiapterin was administered to the 79% gestation (E25) rabbit dam at the start of uterine ischemia. Sepiapterin was dissolved in dimethyl sulfoxide (DMSO) as vehicle and delivered via Alzet osmotic pump (Cupertino, CA) at a dose of 0.6 mg/kg/day and maintained until delivery (~7 days). As controls, a separate subpopulation was administered the vehicle (DMSO) and another subpopulation was administered saline. Saline was used to control for the off-target effects of DMSO. The DMSO and saline groups were combined as controls. All treatment groups (sepiapterin, DMSO or saline) underwent H–I.

2.7. Neurobehavioral studies

The dams were allowed to deliver spontaneously, and a neurobehavioral battery of tests was performed on postnatal day 1, as described before [1]. Neurobehavioral outcomes were compared in newborns between sepiapterin-treated and DMSO- or saline-treated rabbit dams undergoing the same uterine H–I reperfusion protocol. Postural changes and/or hypertonia were classified as a severe outcome, and other mild locomotor effects were classified as mild. Normal kits had no obvious locomotor deficits.

2.8. Experimental design and statistical analysis

Blinding: The investigators performing the biochemical assays and neurobehavioral battery of tests were blinded to the group categorization of fetuses or kits.

Groups: The MRI grouping of fetuses was based on ADC, groups I, II, III, IV. Hypertonia fetuses were groups III or IV, and non-hypertonia fetuses were groups I or II. Newborn kits were grouped as DMSO-, vehicle-, or sepiapterin-treated kits.

Number of Animals: For this animal study, we made sure that we had enough power to discern the effects of the different regions of the fetal brain. The number of fetuses in each group was calculated before the study using a moderate effect size with $\alpha = 0.05$, $\beta = 0.20$, power = 80%.

Descriptive: Tetrahydrobiopterin results were expressed as box and whisker with normal distribution plots, where the box depicts 25th and 75th percentiles, the middle dot is the median, and the whiskers depict the range.

Statistical Methods: An analysis of variance (ANOVA) was used for multiple group comparisons and t-tests were used to determine differences between two groups. Student-Newman-Keuls and Bonferroni post hoc tests were conducted. Bonferroni correction was applied for multiple comparisons. Alpha error was set at $p < 0.05$. Linear and logistic regression were also performed. The 0 h tetrahydrobiopterin level was used as equivalent to *a priori* tetrahydrobiopterin levels. The equalities of the two population correlations and slopes of the lines were tested with Pearson correlation statistics using Fisher's z transformation. For gene expression data, we analyzed Q—Q plots in addition. For all data that did not follow a normal distribution, nonparametric analysis was used.

Structural Equation Modeling: A causal link between tetrahydrobiopterin in various regions with hypertonia was then assessed using path analysis of several possible models by Proc Calis in SAS ver 9.4. Ninety one fetuses had complete data, out of 98 sent for high-powered liquid chromatography–electrochemical detection.

3. Results

3.1. Fetal brain injury predisposition to hypertonia assessed by diffusion-weighted MRI

We used an MRI biomarker to identify the fetuses that are predicted to develop hypertonia or not in the newborn period after undergoing H–I and reperfusion-reoxygenation [3]. Monitoring fetal brain ADC during uterine ischemia, we found four characteristic patterns of change: Pattern I had no change in ADC baseline, Pattern II had a decrease in ADC but above a threshold of 85% of baseline (Fig. 1B), Pattern III had ADC decrease below the threshold, and Pattern IV had ADC during reperfusion period show a subsequent decrease from the ADC level at the end of uterine ischemia (uterine reperfusion, Fig. 1C). The receiver operating characteristic curve for prediction of hypertonia using the presence of either an ADC decrease below the threshold or a subsequent fall in uterine reperfusion (Patterns III or IV) is good to excellent (Fig. 1D). In our study population of 178 fetuses, 16% showed no change, 17% showed a slight fall, 43% fell below the threshold, and 24% had a further fall during uterine reperfusion (Fig. 1E). The sham-operated group showed negligible ADC changes during imaging.

3.2. Individual brain region tetrahydrobiopterin levels and their relationship with hypertonia

To define if tetrahydrobiopterin indicates brain region susceptibility to the development of hypertonia, we conducted a double-blinded study using enough statistical power for moderate effect size similar to a clinical phase III design. We investigated whether susceptibility to hypertonia (as identified by distinct changes in ADC patterns during and

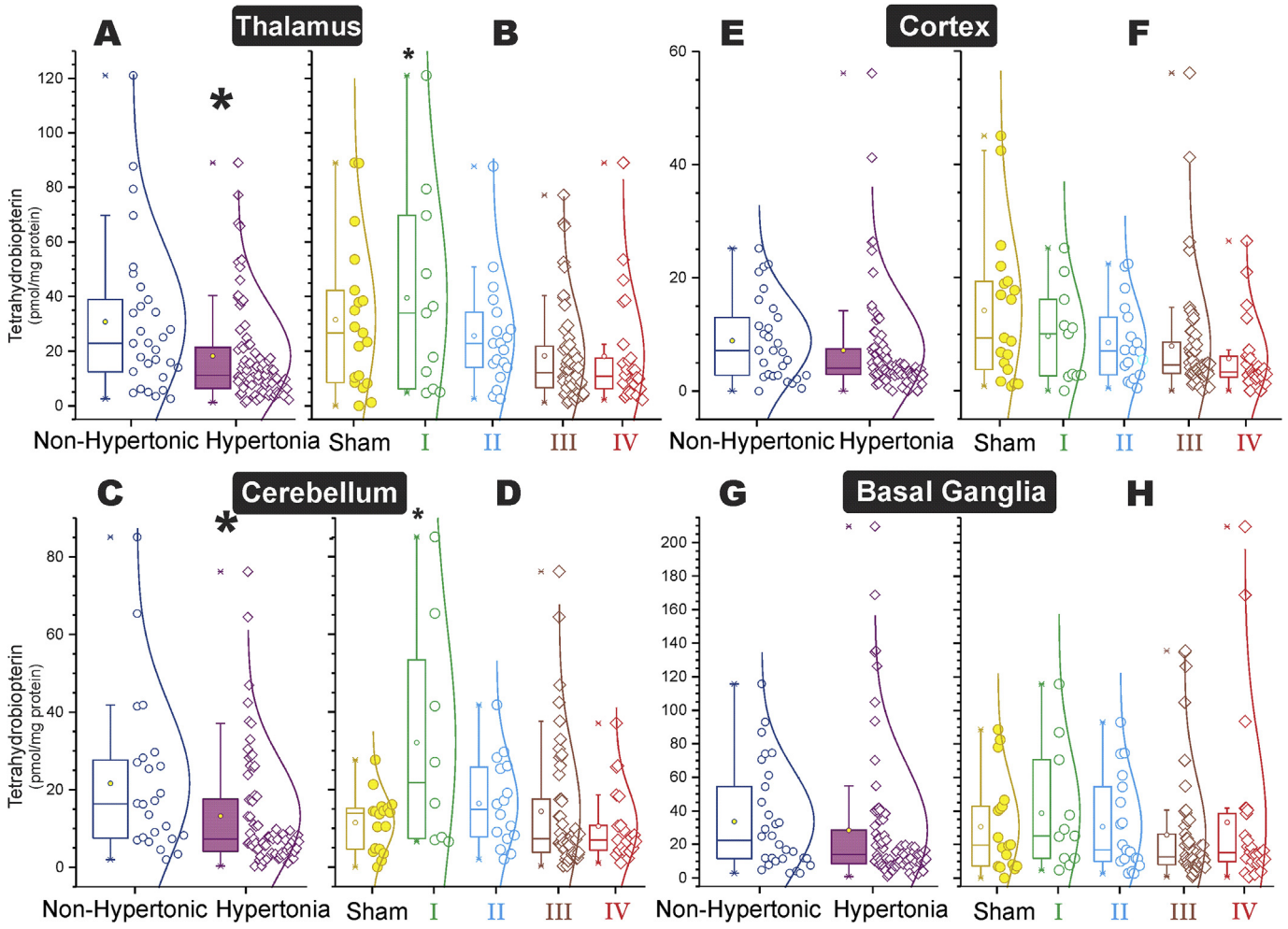

Fig. 2. Tetrahydrobiopterin (BH4) levels in brain regions. Tissue collected immediately after end of H–I/reperfusion period (0 h group) and stratified by MRI patterns. **(A)** Thalamus BH4 is significantly lower in Hypertonia group than Non-Hypertonia (*p < 0.01, two-sample *t*-test, power for actual medium-effect size = 86%). All fetuses underwent H–I. **(B)** Comparing thalamus BH4 in sham (no H–I) with all MRI patterns undergoing H–I, groups are significantly different (*p < 0.05, ANOVA, power for actual medium-large-effect size = 79%). Post hoc tests show pattern I different from patterns III and IV, but not different from sham or pattern II. Patterns III and IV not different from sham or group II (post hoc comparisons with Student-Newman-Keuls multiple range and Bonferroni tests). **(C)** Cerebellum BH4 is significantly lower in Hypertonia group than Non-hypertonia group (*p < 0.05, two-sample *t*-test, power for actual medium-effect size = 68%). **(D)** Comparing cerebellar BH4 in sham with all MRI patterns, groups are significantly different (*p < 0.05, ANOVA, power for actual medium-large-effect size = 80%). Post hoc tests show pattern I different from all other groups (post hoc comparisons with Student-Newman-Keuls and Bonferroni tests). **(E)** Cortex BH4 is not significantly different between hypertonia and Non-hypertonia groups (power for medium-effect size = 74%, for actual effect size = 23%; type II error that the groups are actually different is only 26%). **(F)** Comparing cortex BH4 in sham with all MRI patterns; groups are not significantly different from each other (power for actual effect size = 99%; similarly, type II error is only 1%). **(G)** Basal ganglia BH4 is not significantly different between Hypertonia and Non-hypertonia groups (power for medium-effect size = 75%, for actual effect size = 12%). **(H)** Comparing basal ganglia BH4 in sham with all MRI patterns, groups are not significantly different from each other (power for medium-large-effect size = 79%, for actual effect size = 14%).

after H–I) is influenced by an intrinsic level of tetrahydrobiopterin in the different brain regions. Tetrahydrobiopterin concentration in brain regions was compared between Hypertonia vs No-hypertonia groups as well as between sham and specific MRI Patterns (I, II, III, IV in Fig. 2).

We found that the thalamus and cerebellum showed significant differences in tetrahydrobiopterin levels between Hypertonia (Patterns III and IV) and Non-hypertonia (Patterns I and II (Fig. 2A,C) and in all four MRI Patterns when compared with sham (Fig. 2B,D). The highest concentration of tetrahydrobiopterin was found in the thalamus from Pattern I, a non-hypertonia group, which was distinct from the sham non-H-I group. Note that the tetrahydrobiopterin in Pattern I corresponds to a subpopulation that does not develop hypertonia after H–I, which is the opposite of Patterns III and IV that develop hypertonia after H–I (Fig. 1B and C). The tetrahydrobiopterin levels in the sham group, however, reflect the population values of all rabbits prior to H–I, whether or not they were susceptible to hypertonia. This comparison strongly indicates that susceptibility to H–I injury is dependent on an individual and developmental predisposition to low tetrahydrobiopterin. Tetrahydrobiopterin in the other two regions—cortex and basal ganglia—did not show a difference in Hypertonia vs Non-hypertonia; note the β error of the similarity not being true is as low as 0.01–0.26 (Fig. 2E,G).

3.3. Tetrahydrobiopterin in all brain regions influences hypertonia

We found it interesting that upon further statistical analysis, ANOVA and logistic regression showed that the interaction term of all four regions significantly influenced hypertonia. Since motor disorders can be influenced by the regulation along the basal ganglia and thalamocortical axis, we explored the significance of brain region tetrahydrobiopterin concentrations in Hypertonia and Non-hypertonia groups on the interaction term, or regional connection by analyzing

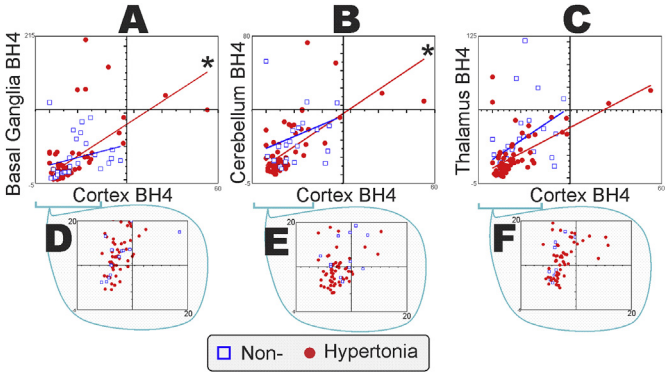

Fig. 3. Regional brain tetrahydrobiopterin (BH4) at 0 h and hypertonia: two-region analysis. A–F. Each data point (either dot or square) is defined by two BH4 values and is unique to one animal. Two-dimensional relationship plots of cortex BH4 with basal ganglia (A), cerebellum (B), and thalamus (C) comparing Hypertonia (filled circles) vs. Non-hypertonia groups (open squares). Correlation between two regions are significant in both groups using Pearson correlation coefficient. **(A)** Cortex BH4 and basal ganglia BH4 correlation for Hypertonia (red line) is different from that in Non-hypertonia (blue linear regression lines, note difference in slopes). Pearson correlation coefficient transformed into a Fisher's z score and statistically compared between Hypertonia and Non-hypertonia. **(B)** Cortex BH4 and cerebellum BH4 correlation for Hypertonia (red line) is different from that in Non-hypertonia (blue line); linear regression lines shown. **(C)** Other correlations of two regions between Hypertonia and Non-Hypertonia groups were not significant including between cortex BH4 and thalamus BH4, shown here. **(D–F)** Depicted in D–F are the correlation for values arbitrarily chosen to be ≤ 20 pmol/mg protein. D corresponds to A, E to B, and F to C. At low BH4 levels, in the basal ganglia, cerebellum, or thalamus (depicted in the ordinate) predisposes to hypertonia for any value of BH4 in cortex. More red dots (Hypertonia) than blue open squares (Non-hypertonia) in the lower left quadrant, indicates that at really low BH4 levels, a low BH4 level in two regions may still predispose a fetus to hypertonia. (For interpretation of the references to color in this figure legend, the reader is referred to the Web version of this article.)

two-, three-, and four-brain regions. Interactions of two brain regions were then assessed by investigating the equality of the Pearson correlations with Fisher's z transformation, comparing Hypertonia and Non-hypertonia groups. In this analysis, the cortex and cerebellum and the cortex and basal ganglia were significantly different among all two-region comparisons (Fig. 3A and B), indicating predisposition to hypertonia in the interaction of two-regions. The thalamus was not significantly different from the other regions (only the cortex correlation is shown in Fig. 3C). However, low tetrahydrobiopterin levels (< 20 pmol/mg protein) in any of the regions, basal ganglia, cerebellum, or thalamus combined with a low cortex level predisposes to hypertonia (Fig. 3D–F).

Interactions of all combinations of the three regions were significantly associated with Hypertonia in univariate analysis. Expanding the analysis to three brain regions, three-dimensional plots with three-region-correlations showed emergence of noticeably different planes between Hypertonia and Non-hypertonia groups (cortex-basal ganglia-cerebellum in Fig. 4A and B and thalamus-cortex-cerebellum in Fig. 4C and D).

We also investigated whether gender and brain region influence hypertonia in a univariate analysis. The highest tetrahydrobiopterin levels were always seen in non-hypertonic males, possibly weakly indicating that a subpopulation of males may be protected from hypertonia by high tetrahydrobiopterin levels (Fig. 5).

Additional analyses of the relationship between the tetrahydrobiopterin variations in all four brain regions as a causal factor of injury using structural equation modeling indicated the relative contribution of four brain regions as a cause of hypertonia. The best model obtained with path analysis (Fig. 6) confirms that thalamus

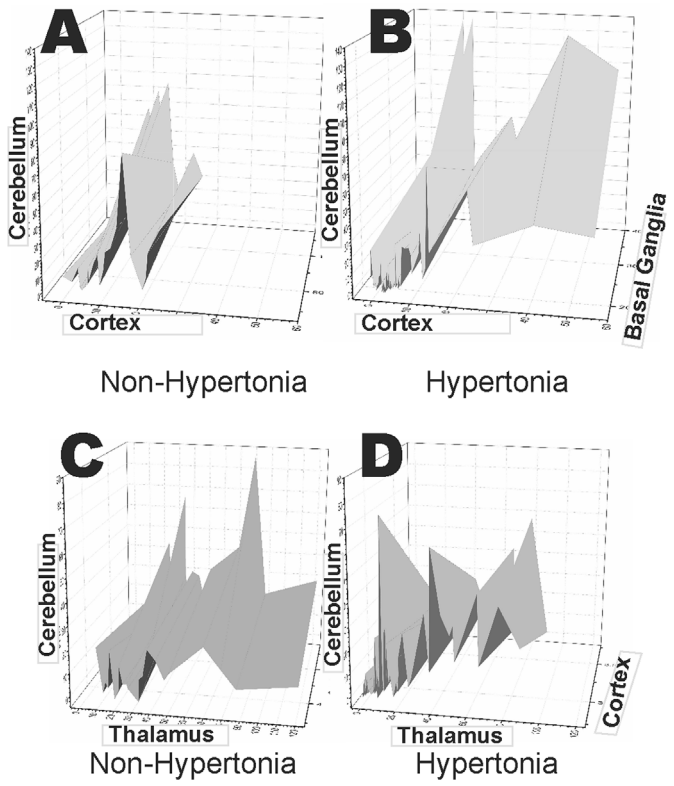

Fig. 4. Influence of brain region tetrahydrobiopterin (BH4) at 0 h and hypertonia. Three-dimensional plots showing differences in the BH4 of three brain regions; (B,D) compare hypertonia and (A,C) compare non-hypertonia. A and B show the X-axis as cortex BH4, Y-axis as basal ganglia BH4, and Z-axis as cerebellum BH4. C and D show the X-axis as thalamus BH4, Y-axis as cortex BH4, and Z-axis as cerebellum BH4. The plots are different for hypertonia compared with non-hypertonia when any three regions are selected and compared.

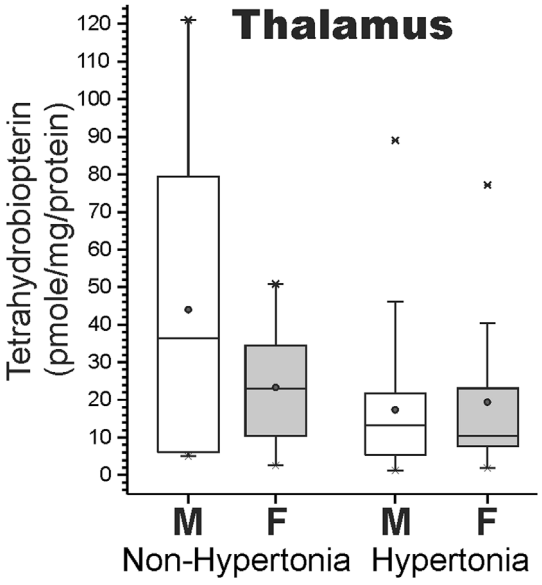

Fig. 5. Gender as a factor in tetrahydrobiopterin and susceptibility to hypertonia. Box-and-whisker plots show thalamus BH4, with no statistical difference between males and females when compared between the hypertonia and non-hypertonia groups (two-way ANOVA; power for actual medium-large effect size = 82%). Note that a subpopulation of males with high tetrahydrobiopterin do not develop hypertonia.

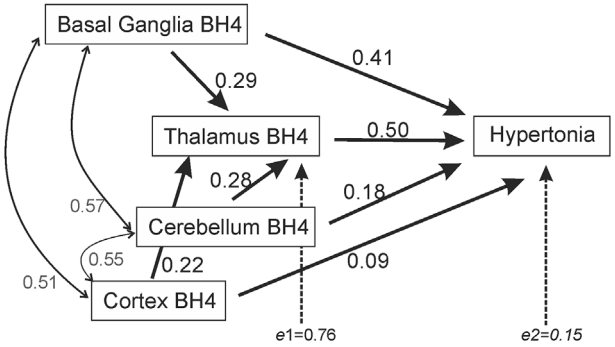

Fig. 6. Influence of brain region tetrahydrobiopterin (BH4) at 0 h and hypertonia. Path analysis using structural equation modeling with the best fit from various models using all four regional BH4 values causing hypertonia. The other three regions have both direct and indirect effects through thalamus BH4. Black shows coefficients of the direct effect, gray shows covariance effects, and black italcs shows errors to the path (e1 and e2). The overall model has absolute Chi-square of 0.0000, Goodness of Fit Index of 1.000, Akaike Information Criterion 28, Schwarz Bayesian Criterion 63, and Bentler Comparative Fit Index of 0.9668 using Proc Calis in SAS.

tetrahydrobiopterin has the strongest effect on Hypertonia. The other three regions have both a direct and an indirect effect on Hypertonia through the thalamus. What is remarkable is that the error for thalamic tetrahydrobiopterin influence on Hypertonia in this best-fit model is 0.15 implying that the score reliability coefficient is high.

3.4. Gene expression of enzymes of tetrahydrobiopterin pathway do not explain differences in tetrahydrobiopterin levels

To investigate whether decreased gene expression of enzymes involved in the tetrahydrobiopterin pathway explain the individual low brain region levels, we investigated specific gene expression levels in the thalamus, cerebellum, and cortex (n = 6 for each MRI pattern). The analysis included enzymes involved in *de novo* synthesis (GTP cyclohydrolase I [GTPCH-1], 6-pyruvoyltetrahydropterin synthase [PTPS], and SPR, recycling (DHPR), and salvage pathways (DHFR). We found no direct association between biosynthetic enzyme gene expressions and tetrahydrobiopterin levels (Fig. 7) or recycling and salvage pathway enzymes (not shown).

3.5. Low gene expression of enzymes of tetrahydrobiopterin pathway are not high risk for hypertonia

The actual gene expression of biosynthetic enzymes was not significantly different between Hypertonia and Non-hypertonia groups (Fig. 7B and C), indicating that factors other than gene expression control basal endogenous tetrahydrobiopterin neuroprotective levels.

3.6. Reactive nitrogen species is a possible mechanistic factor

Since changes in the cortex were associated with development of hypertonia (Figs. 4 and 6) we hypothesized that the cortex may become a target of oxidant injury upon tetrahydrobiopterin loss in other brain regions. Protein nitrotyrosine is associated with brain injury and increased superoxide formation as we have shown to occur in H–I reperfusion. We analyzed nitrotyrosine changes in cortex samples with the automated Western blot method, which provides a standardized assessment of samples (Fig. 8A). Our analysis showed increased levels in the cortex of hypertonia group compared with the non-hypertonia group (Fig. 8B and C). This finding indicates that oxidant injury resulting from H–I likely propagates injury through mechanisms involving reactive nitrogen species.

4. Tetrahydrobiopterin changes after hypoxia-ischemia and reperfusion

Tetrahydrobiopterin depletion immediately after H–I (0 h) may increase cell death or cellular dysfunction. In either case, it would be expected that tetrahydrobiopterin depletion is further aggravated at later times from H–I in the same neurons. As described before (Fig. 1), another group of rabbit dams were delivered by C-section 48 hr after H–I. In this 48-hr group, analysis of tetrahydrobiopterin levels in the different brain regions, in the groups with MRI patterns predictive of hypertonia (patterns III and IV) were found not to be different from those of non-hypertonia (Fig. 9A,C,E,G). Comparing tetrahydrobiopterin in sham-operated with various MRI patterns, groups are significantly different for only the cortex (Fig. 9F) and thalamus (Fig. 9G).

These results confirmed that H–I causes long-lasting effects, although the delayed tetrahydrobiopterin responses did not recapitulate the initial (0 h) depletion in the hypertonia group. Rather, these results

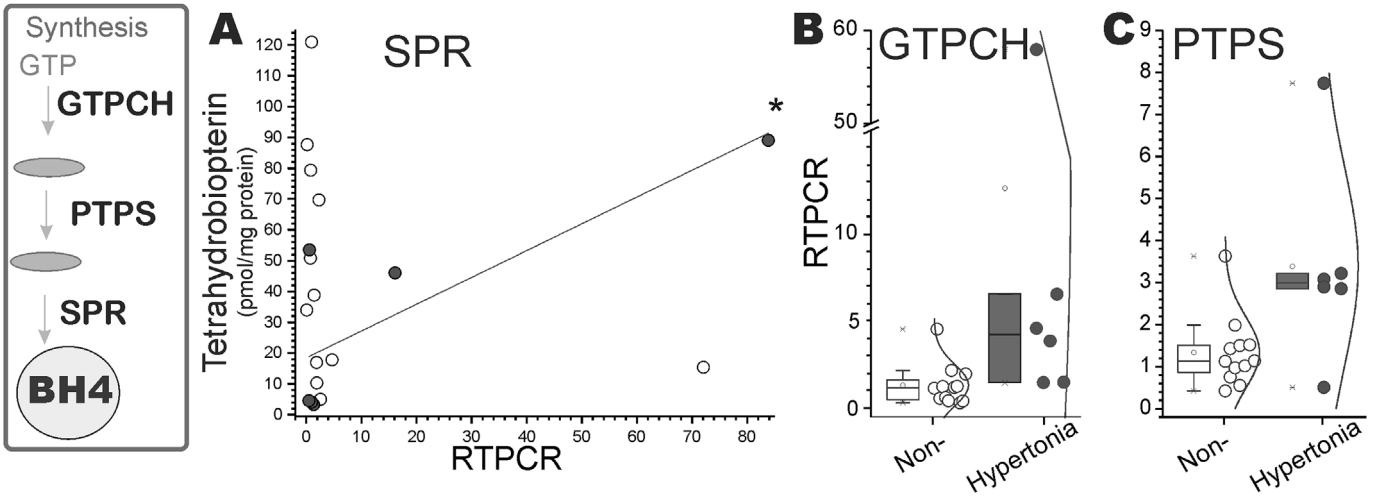

Fig. 7. Gene expression of tetrahydrobiopterin (BH4) enzymes. Expression of mRNA was analyzed in brain regions showing low or high BH4. Identification of genes for rabbit BH4 biosynthetic and regeneration enzymes was performed. **(A)** Correlation of thalamus BH4 with SPR only in the Hypertonia group (filled dots) vs. Non-hypertonia (open dots), p = 0.0472. No significant correlation in Non-hypertonia group. **(B)**. Comparison between Non-hypertonia and Hypertonia groups did not show any difference with any of the enzymes except for GTPCH-1 (Wilcoxon two-sample test, p = 0.0076) and in **(C)** for PTPS (p = 0.0549). Because of multiple comparisons and Bonferroni correction, these were not considered significant.

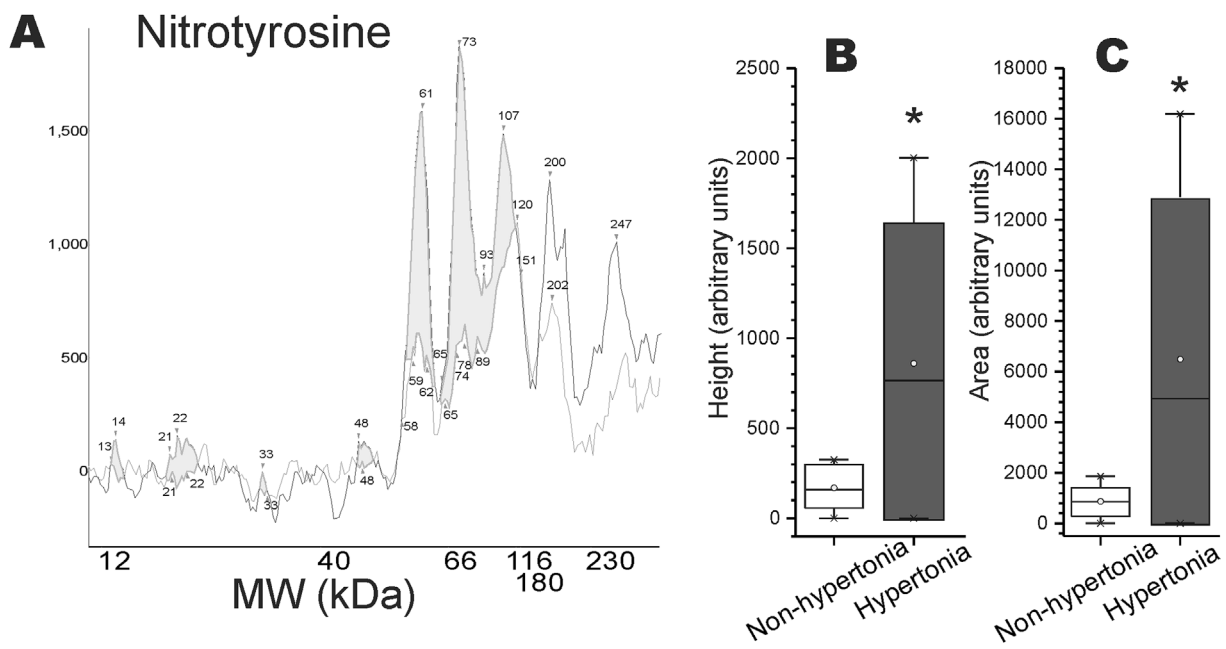

Fig. 8. Nitrotyrosine formation in cortex. (A). Chromatogram of automated Western blot showing nitrotyrosine formation by the difference between blocked antibody (negative control, gray lower line on right half) and unblocked antibody (black). Shaded highlighted portion shows proteins that have specific binding to nitrotyrosine. **(B, C)** The cortex was the only region analyzed because of tissue availability. Increase in cortex nitrotyrosine formation in the Hypertonia group compared with the Non-hypertonia group using height (B) or area (C) of the scan peaks; Wilcoxon two-sample test, n = 6–8/group, *p < 0.05.

indicate that delayed responses are most likely reactive responses to the initial H–I, involving different parts of the brain.

4.1. Replenishing tetrahydrobiopterin immediately after injury prevents further brain injury

Because increasing tetrahydrobiopterin during the late (48 h) reactive process may be inadequate to protect against brain injury, we asked whether elevating tetrahydrobiopterin levels soon after injury could be a strategy to prevent damage in the brain. To this end, dams were treated with sepiapterin, a precursor of tetrahydrobiopterin, using an osmotic pump immediately after H–I-reperfusion injury. This intervention was successful at decreasing deaths and increasing the number of normal functioning kits (Fig. 10). The decrease in deaths did also come with an increase of severely affected kits.

5. Discussion

One important dilemma in determining mechanisms of fetal neuropathology is that not all subjects respond the same to a hypoxic event. This is clearly exemplified in animal models, which were exposed to same level of hypoxia under well-controlled conditions, not all fetuses in the litter developed same impairment; rather, a pattern of response emerged. Our studies demonstrate that the degree of brain response to injury could be explained by endogenous neuronal factors. Our analysis indicates that the susceptibility to fetal brain H–I-reperfusion injury is determined by individual variation and combinations of brain regional tetrahydrobiopterin levels, in contrast to only one specific brain region or a specific global low threshold level of tetrahydrobiopterin. To the same level of insult, a fetus can develop hypertonia or not based on the combinations of tetrahydrobiopterin levels found in different brain regions. Thus, a paradigm-shift in understanding the predisposition to H–I injury at prematurity and subsequent development of hypertonia is proposed. Tetrahydrobiopterin deficiency *per se* and in different degrees is known to result in movement disorders in children [5,12], but for hypertonia, it appears to be influenced by specific regional deficiency. Structural equation modeling helped elucidate the multi-dimensional role played by different regions in an *in vivo* animal model. The consequences of tetrahydrobiopterin deficiency in biochemical terms would be a decrease in the production of monoamine neurotransmitters (dopamine, serotonin), a decrease in nitric oxide, and NOS-uncoupling resulting in enhanced superoxide.

An important advance in identifying the role of tetrahydrobiopterin in the mechanism of the H–I-induced hypertonia was the use of the MRI surrogate biomarker that resolves the dilemma of studying *early* H–I events with *later-onset* hypertonia. We would not be able to differentiate between the fetuses who would have developed hypertonia from those with a normal muscle tone for tissue taken early, such as at 0 h and 48 h if we did not have MRI to guide us. In our initial studies without the use of MRI [8], thalamus obtained after H–I at 70% gestation (E22) showed tetrahydrobiopterin loss, but the specificity of tetrahydrobiopterin depletion with respect to H–I-injury could not be determined, as not all newborns showed the same phenotype following antenatal H–I. Also, tissue taken at the time of diagnosis of hypertonia (in our case after birth), would miss the fact that there is an intrinsic predisposing low level of tetrahydrobiopterin. We show that by 48 h, there was little to differentiate tetrahydrobiopterin levels in parts of the brain from Hypertonia and Non-Hypertonia groups.

Tetrahydrobiopterin levels in both thalamus and cerebellum in MRI group I (Non-hypertonia group) are significantly higher than in groups III and IV (Hypertonia groups). In cerebellum, Group I levels are higher than sham. The implication is that in the normal population (represented by sham) there is a range of low and high tetrahydrobiopterin levels; albeit in fetuses, all these levels are lower than postnatal levels. Those fetuses at the higher end of the normal distribution i.e. high tetrahydrobiopterin level are more likely to escape becoming hypertonic when subjected to H–I. Fetuses at the lower end of the normal distribution are more susceptible to becoming hypertonic and show a combination of low tetrahydrobiopterin in brain regions particularly in the thalamus. Some of the low-tetrahydrobiopterin fetuses in the Sham group would become Group III or IV if subjected to H–I. It is important to note that a relatively low level of tetrahydrobiopterin *per se* probably does not cause hypertonia, but a high level confers some resistance to becoming hypertonic. The present study is thus important in

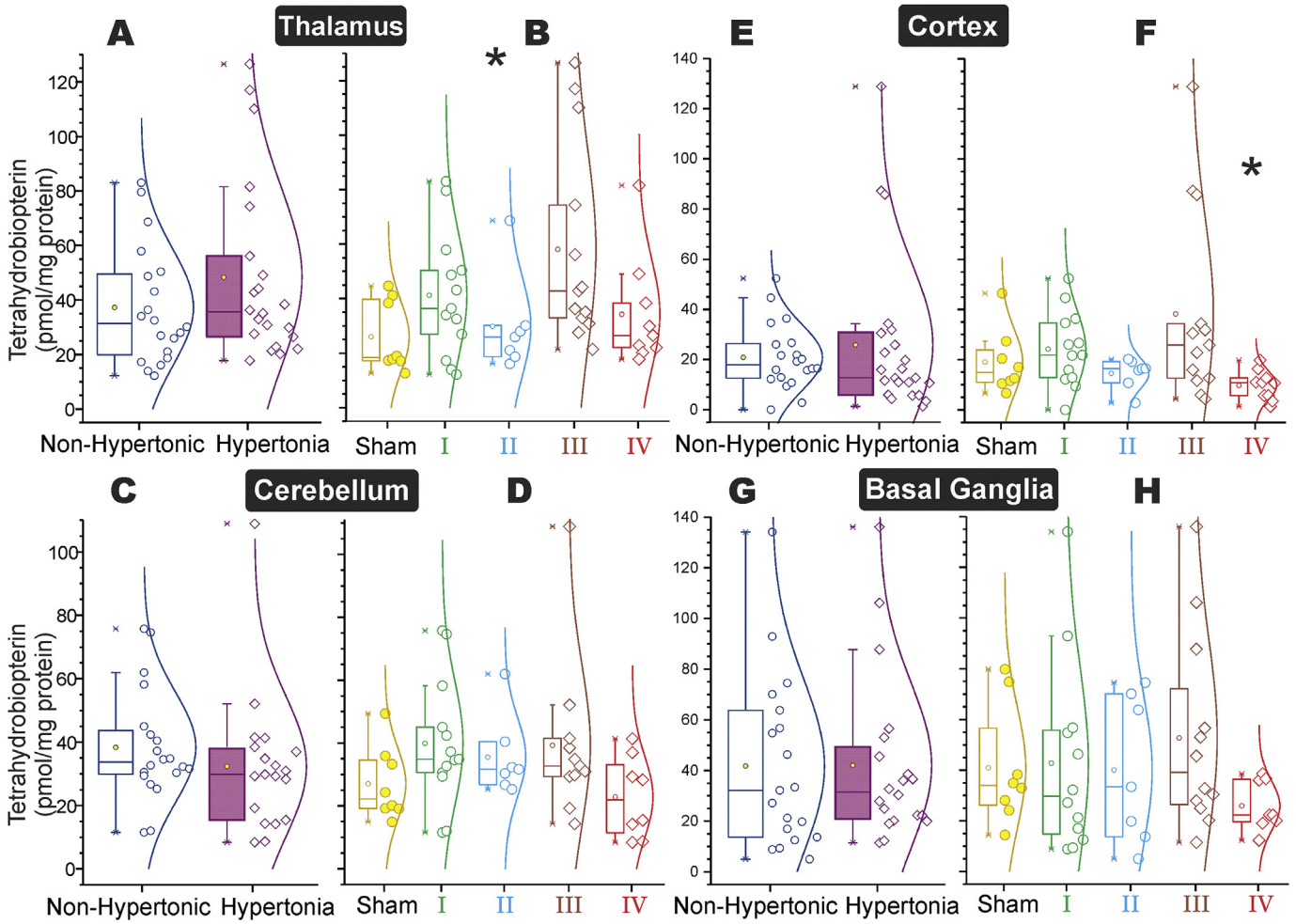

Fig. 9. Tetrahydrobiopterin in brain regions 48 h after H–I: Regional BH4 analysis in hypertonia and non-hypertonia groups **(A,C,E,G)** and MRI patterns and sham **(B,F,D,H)**. No significant difference was found between hypertonia and non-hypertonia groups. The powers of two-sample *t*-test for medium effect size were: thalamus 48% (A), cerebellum 45% (C), cortex 48% (E), and basal ganglia 45% (G). Comparing sham with various MRI patterns, groups are significantly different for cortex (F) and thalamus (B); *$p < 0.05$, ANOVA, powers for actual large effect size = 64% and 63%, respectively. Student-Newman-Keuls and Bonferroni post hoc tests showed a difference in the cortex only for MRI groups I & II and sham vs. II, III, IV and sham (F). Comparing sham with various MRI patterns, the cerebellum (D) and basal ganglia (H) were not different between groups; powers for actual medium-large effect size 41% and 28%, respectively.

establishing that the endogenous tetrahydrobiopterin level before H–I in different regions is associated with susceptibility/resistance to an insult.

After 48 h of H–I injury, tetrahydrobiopterin levels were not different between Hypertonia and Non-hypertonia groups. Only in the Sham group, there was a significant increase in cerebellar tetrahydrobiopterin at 48 h compared to 0 h. By 48 h it is possible that brain regions recovered from the loss of tetrahydrobiopterin from oxidants, or other secondary responses to H–I such as inflammation affected tetrahydrobiopterin levels. We verified that tetrahydrobiopterin significantly increased 48 h after H–I, most notably, only in the group with MRI pattern III in all four brain regions and is exemplified by changes in the thalamus (18.3 ± 2.5 to 58.1 ± 10.2 pmol/mg protein, $p < 0.0001$). This indicates that the mechanisms of responsive increase in tetrahydrobiopterin are most likely regulated by the degree of injury. H–I alone could cause an increase in the microglia and a release of inflammatory mediators [13]. Plasma inflammatory cytokines are increased in neonatal encephalopathy, mostly derived from H–I [14,15]. Microglial aggregation in the dentate gyrus is observed in various human scenarios of perinatal H–I [16]. Cerebral ischemia in deep hypothermia during newborn cardiac surgery elicits an immediate innate inflammatory response [17]. A possible explanation for our findings could be that oxidants are involved and cause an increase in inflammatory response, as has been suggested by ethanol toxicity models [18]. Some of the inflammatory components are recognized stimulators of tetrahydrobiopterin synthesis [19]. A reactive response causing an increase in tetrahydrobiopterin to protect against oxidant damage cannot be ruled out. This is suggested by significant increases in pattern IV in the thalamus and cerebellum, albeit with less magnitude (18.2 ± 3.9 to 34.2 ± 6.8 pmol/mg protein in thalamus, $p = 0.046$).

The gene expression studies did not elucidate if biosynthetic and/or regeneration enzymes explained the developmental variations in tetrahydrobiopterin across different brain regions. It would be interesting, however, to investigate in human subjects how the polymorphism of the enzymes in the tetrahydrobiopterin pathway influences H–I brain injury and motor deficits.

5.1. *Tetrahydrobiopterin as a therapeutic strategy*

Preventing or minimizing early tetrahydrobiopterin depletion in H–I-reperfusion injury has a significant neuroprotective impact. Treatment with tetrahydrobiopterin precursor, sepiapterin, prior to H–I in the brain at E22 improves motor outcomes and overall survival rates [8]. In this study, we showed that treatment after H–I-reperfusion is also moderately beneficial. It is likely that tetrahydrobiopterin

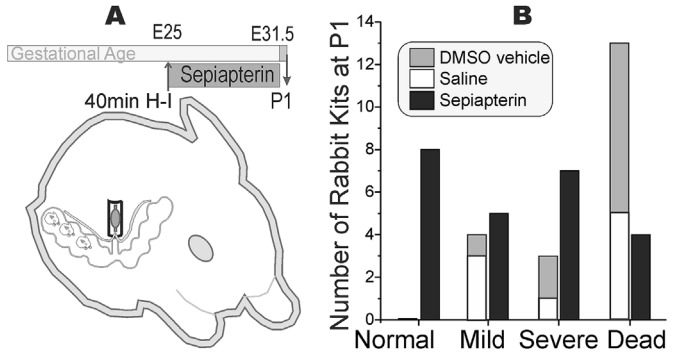

Fig. 10. Sepiapterin treatment post H–I prevents severe hypertonia and death. (A) Sepiapterin administration to pregnant dams after start of 40-min uterine ischemia at 79% gestation (E25) through delivery of fetuses at E31.5. Neurobehavioral battery done at P1 (E32). **(B)** Sepiapterin was compared to its vehicle (DMSO) as well as saline controls in view of DMSO's possible off-target effects. Abscissa shows gross classification of neurobehavior (hypertonia or postural changes classified as severe) and ordinate shows the number of kits at P1. Each animal is counted in its own group, whether DMSO, saline or sepiapterin treatment. DMSO (gray bars) and saline (white bars) were combined as controls because they were not different. Black bars indicate sepiapterin treated kits. Sepiapterin treatment increases the number of normal kits and decreases the number of dead kits. It is possible that some of the dead kits saved by sepiapterin contribute to the increase in the severe outcome.

improves NOS uncoupling and increasing nitric oxide production. Elevated reactive oxygen species as a mechanism is concordant with our previous experimental evidence showing that antioxidant treatments such as superoxide dismutase mimetics, ascorbate, and/or trolox are also beneficial [3,20]. Although we have not shown those treatments to prevent tetrahydrobiopterin depletion, they decrease oxidant injury and potentially also downstream oxidative modifications. Whether a sole effect of reactive oxygen species on tetrahydrobiopterin during H–I could explain the depletion of tetrahydrobiopterin measured at 0 h cannot be definitively established in our experimental setting. This effect is unlikely in this case because we didn't find more depletion of tetrahydrobiopterin in Group IV (reperfusion reoxygenation), where we know more reactive oxygen species is produced, compared to Group III (end H–I).

Interventions to ameliorate H–I-reperfusion injury are urgently needed. New biomarkers of preterm and term H–I injuries are emerging [15,21], but there are just too few options for clinical treatments. Cooling for term neonatal encephalopathy has become a standard therapy in neonatal intensive care units [22–27], but improvement in death or disability is only ~15%. Because magnesium sulfate is the only therapy available for premature brain injury resulting in CP [28], tetrahydrobiopterin may be a promising new therapy for premature and near-term brain injury.

The present study also explains the discrepancy of *ex vivo* survival of neuronal cells isolated from different brain regions being unrelated to the differences in endogenous levels in our previous publication [9]. Based on tetrahydrobiopterin levels, the E22 thalamus neurons at 70% gestation were expected to show increased resistance to H–I injury compared to cortical neurons with a comparatively lower tetrahydrobiopterin content. The E22 thalamus, however, was more sensitive to death than the cortex. As expected, the E29 thalamus with higher tetrahydrobiopterin levels was much more resistant to H–I than the E22 thalamus, which also showed improved survival rates upon tetrahydrobiopterin supplementation [9]. Previously, we thought that a general low or depleted tetrahydrobiopterin levels explained increased oxidant production [29–31]. Downstream responses such as disturbances in mitochodrial metabolic activity and changes in calcium buffering results in an amplified response to hypoxia [32,33]. This thinking needed to be adjusted to account for the possibility that the initiating threshold may be different depending on the regional tetrahydrobiopterin levels. The advantage of high endogenous tetrahydrobiopterin is that the initial oxidation of the cofactor will have a lesser impact in the overall downstream events preventing NOS uncoupling and reactive oxygen species release [10]. NOS-uncoupling consequences may explain the fact that increased tetrahydrobiopterin content prevents H–I reperfusion injury, as shown in the brains that are refractory to the same level of H–I reperfusion injury. In our previous studies, we demonstrated that a higher level of superoxide radical anion production occurs in the period of reperfusion–reoxygenation, Group IV [3].

One limitation of the study is that we could not show low tetrahydrobiopterin to correlate with reactive nitrogen species as there was not enough tissue from an individual fetus to run multiple biochemical assays, especially in the thalamus, basal ganglia, and cerebellum. Combining tissues from different animals is a possibility; however, that does not take into account that tissue damage from reactive nitrogen species is often locally circumscribed and, thus, variations from animal to animal would not be accounted for. The technological challenges of assaying tetrahydrobiopterin and reactive nitrogen species in smaller regions of interest such as at a cellular level may be solved in the future.

6. Conclusions

The predisposition to hypertonia in certain premature fetuses is dependent on regional brain tetrahydrobiopterin levels. When subjected to H–I, certain fetuses with decreased tetrahydrobiopterin levels developed critical brain injury and developed hypertonia postnatally; other fetuses with optimal tetrahydrobiopterin levels did not. In this regional etiological factor, thalamic tetrahydrobiopterin plays a dominant role. These conclusions could only be achieved by performing an animal study with sufficient power to characterize the role of the tetrahydrobiopterin levels in two-, three- and four-brain regions on hypertonia development. Furthermore, tetrahydrobiopterin supplementation may be considered as a possible neuroprotectant, even when administered after H–I. The mechanisms of protection may be through the amelioration of oxidative modifications induced by reactive nitrogen species.

Declaration of competing interest

None other than support by grants from the National Institute of Neurological Disorders and Stroke, National Institutes of Health, USA under grant numbers R01 NS081936 (Vasquez-Vivar, Tan) and R56 NS100088 (Tan).

Acknowledgements

This work was supported by the National Institute of Neurological Disorders and Stroke, National Institutes of Health, USA under grant numbers R01 NS081936 (Vasquez-Vivar, Tan) and R56 NS100088 (Tan).

Appendix A. Supplementary data

Supplementary data to this article can be found online at https://doi.org/10.1016/j.redox.2019.101407.

References

[1] M. Derrick, N.L. Luo, J.C. Bregman, T. Jilling, X. Ji, K. Fisher, C.L. Gladson, D.J. Beardsley, G. Murdoch, S.A. Back, S. Tan, Preterm fetal hypoxia-ischemia causes hypertonia and motor deficits in the neonatal rabbit: a model for human cerebral palsy? J. Neurosci. 24 (2004) 24–34.

[2] A. Drobyshevsky, M. Derrick, P.V. Prasad, X. Ji, I. Englof, S. Tan, Fetal brain magnetic resonance imaging response acutely to hypoxia-ischemia predicts postnatal outcome, Ann. Neurol. 61 (2007) 307–314.

[3] A. Drobyshevsky, K. Luo, M. Derrick, L. Yu, H. Du, P.V. Prasad, J. Vasquez-Vivar, I. Batinic-Haberle, S. Tan, Motor deficits are triggered by reperfusion-reoxygenation injury as diagnosed by MRI and by a mechanism involving oxidants, J. Neurosci. 32 (2012) 5500–5509.
[4] L. Elzaouk, W. Leimbacher, M. Turri, B. Ledermann, K. Burki, N. Blau, B. Thony, Dwarfism and low insulin-like growth factor-1 due to dopamine depletion in Pts-/- mice rescued by feeding neurotransmitter precursors and H4-biopterin, J. Biol. Chem. 278 (2003) 28303–28311.
[5] H. Shintaku, Disorders of tetrahydrobiopterin metabolism and their treatment, Curr. Drug Metabol. 3 (2002) 123–131.
[6] J. Vasquez-Vivar, N. Hogg, P. Martasek, H. Karoui, K.A. Pritchard Jr., B. Kalyanaraman, Tetrahydrobiopterin-dependent inhibition of superoxide generation from neuronal nitric oxide synthase, J. Biol. Chem. 274 (1999) 26736–26742.
[7] J. Vasquez-Vivar, B. Kalyanaraman, P. Martasek, N. Hogg, B.S. Masters, H. Karoui, P. Tordo, K.A. Pritchard Jr., Superoxide generation by endothelial nitric oxide synthase: the influence of cofactors, Proc. Natl. Acad. Sci. U. S. A. 95 (1998) 9220–9225.
[8] J. Vasquez-Vivar, J. Whitsett, M. Derrick, X. Ji, L. Yu, S. Tan, Tetrahydrobiopterin in the prevention of hypertonia in hypoxic fetal brain, Ann. Neurol. 66 (2009) 323–331.
[9] L. Yu, J. Vasquez-Vivar, R. Jiang, K. Luo, M. Derrick, S. Tan, Developmental susceptibility of neurons to transient tetrahydrobiopterin insufficiency and antenatal hypoxia-ischemia in fetal rabbits, Free Radic. Biol. Med. 67 (2014) 426–436.
[10] J. Vasquez-Vivar, Z. Shi, K. Luo, K. Thirugnanam, S. Tan, Tetrahydrobiopterin in antenatal brain hypoxia-ischemia-induced motor impairments and cerebral palsy, Redox Biol. 13 (2017) 594–599.
[11] Z. Shi, J. Vasquez-Vivar, K. Luo, Y. Yan, F. Northington, M. Mehrmohammadi, S. Tan, Ascending lipopolysaccharide-induced intrauterine inflammation in near-term rabbits leading to newborn neurobehavioral deficits, Dev. Neurosci. (2019) 1–13.
[12] L. Jaggi, M.R. Zurfluh, A. Schuler, A. Ponzone, F. Porta, L. Fiori, M. Giovannini, R. Santer, G.F. Hoffmann, H. Ibel, U. Wendel, D. Ballhausen, M.R. Baumgartner, N. Blau, Outcome and long-term follow-up of 36 patients with tetrahydrobiopterin deficiency, Mol. Genet. Metab. 93 (2008) 295–305.
[13] C. Mallard, J.O. Davidson, S. Tan, C.R. Green, L. Bennet, N.J. Robertson, A.J. Gunn, Astrocytes and microglia in acute cerebral injury underlying cerebral palsy associated with preterm birth, Pediatr. Res. 75 (2014) 234–240.
[14] V. Chaparro-Huerta, M.E. Flores-Soto, M.E. Merin Sigala, J.C. Barrera de Leon, M.L. Lemus-Varela, B.M. Torres-Mendoza, C. Beas-Zarate, Proinflammatory cytokines, enolase and S-100 as early biochemical indicators of hypoxic-ischemic encephalopathy following perinatal asphyxia in newborns, Pediatr. Neonatol. 58 (2017) 70–76.
[15] A.N. Massaro, Y.W. Wu, T.K. Bammler, B. Comstock, A. Mathur, R.C. McKinstry, T. Chang, D.E. Mayock, S.B. Mulkey, K. Van Meurs, S. Juul, Plasma biomarkers of brain injury in neonatal hypoxic-ischemic encephalopathy, J. Pediatr. 194 (2018) 67–75 e61.
[16] M.R. Del Bigio, L.E. Becker, Microglial aggregation in the dentate gyrus: a marker of mild hypoxic-ischaemic brain insult in human infants, Neuropathol. Appl. Neurobiol. 20 (1994) 144–151.
[17] S.O. Algra, K.M. Groeneveld, A.W. Schadenberg, F. Haas, F.C. Evens, J. Meerding, L. Koenderman, N.J. Jansen, B.J. Prakken, Cerebral ischemia initiates an immediate innate immune response in neonates during cardiac surgery, J. Neuroinflammation 10 (2013) 24.
[18] F. Akhtar, C.A. Rouse, G. Catano, M. Montalvo, S.L. Ullevig, R. Asmis, K. Kharbanda, S.K. Maffi, Acute maternal oxidant exposure causes susceptibility of the fetal brain to inflammation and oxidative stress, J. Neuroinflammation 14 (2017) 195.
[19] A. Chiarini, I. Dal Pra, R. Gottardo, F. Bortolotti, J.F. Whitfield, U. Armato, BH(4) (tetrahydrobiopterin)-dependent activation, but not the expression, of inducible NOS (nitric oxide synthase)-2 in proinflammatory cytokine-stimulated, cultured normal human astrocytes is mediated by MEK-ERK kinases, J. Cell. Biochem. 94 (2005) 731–743.
[20] M. Derrick, J. He, E. Brady, S. Tan, The in vitro fate of rabbit fetal brain cells after acute in vivo hypoxia, J. Neurosci. 21 (2001) RC138.
[21] E.M. Graham, A.D. Everett, J.C. Delpech, F.J. Northington, Blood biomarkers for evaluation of perinatal encephalopathy: state of the art, Curr. Opin. Pediatr. 30 (2018) 199–203.
[22] W.H. Zhou, G.Q. Cheng, X.M. Shao, X.Z. Liu, R.B. Shan, D.Y. Zhuang, C.L. Zhou, L.Z. Du, Y. Cao, Q. Yang, L.S. Wang, G. China Study, Selective head cooling with mild systemic hypothermia after neonatal hypoxic-ischemic encephalopathy: a multicenter randomized controlled trial in China, J. Pediatr. 157 (2010) 367–372 372 e361–363.
[23] G. Simbruner, R.A. Mittal, F. Rohlmann, R. Muche, Systemic hypothermia after neonatal encephalopathy: outcomes of neo.nEURO.network RCT, Pediatrics 126 (2010) e771–778.
[24] P.D. Gluckman, J.S. Wyatt, D. Azzopardi, R. Ballard, A.D. Edwards, D.M. Ferriero, R.A. Polin, C.M. Robertson, M. Thoresen, A. Whitelaw, A.J. Gunn, Selective head cooling with mild systemic hypothermia after neonatal encephalopathy: multicentre randomised trial, Lancet 365 (2005) 663–670.
[25] S. Shankaran, A.R. Laptook, R.A. Ehrenkranz, J.E. Tyson, S.A. McDonald, E.F. Donovan, A.A. Fanaroff, W.K. Poole, L.L. Wright, R.D. Higgins, N.N. Finer, W.A. Carlo, S. Duara, W. Oh, C.M. Cotten, D.K. Stevenson, B.J. Stoll, J.A. Lemons, R. Guillet, A.H. Jobe, H. National Institute of Child, N. Human Development Neonatal Research, Whole-body hypothermia for neonates with hypoxic-ischemic encephalopathy, N. Engl. J. Med. 353 (2005) 1574–1584.
[26] D.V. Azzopardi, B. Strohm, A.D. Edwards, L. Dyet, H.L. Halliday, E. Juszczak, O. Kapellou, M. Levene, N. Marlow, E. Porter, M. Thoresen, A. Whitelaw, P. Brocklehurst, T.S. Group, Moderate hypothermia to treat perinatal asphyxial encephalopathy, N. Engl. J. Med. 361 (2009) 1349–1358.
[27] S.E. Jacobs, C.J. Morley, T.E. Inder, M.J. Stewart, K.R. Smith, P.J. McNamara, I.M. Wright, H.M. Kirpalani, B.A. Darlow, L.W. Doyle, C. Infant Cooling Evaluation, Whole-body hypothermia for term and near-term newborns with hypoxic-ischemic encephalopathy: a randomized controlled trial, Arch. Pediatr. Adolesc. Med. 165 (2011) 692–700.
[28] C.A. Crowther, P.F. Middleton, M. Voysey, L. Askie, L. Duley, P.G. Pryde, S. Marret, L.W. Doyle, A. Group, Assessing the neuroprotective benefits for babies of antenatal magnesium sulphate: an individual participant data meta-analysis, PLoS Med. 14 (2017) e1002398.
[29] J. Vasquez-Vivar, J. Whitsett, P. Martasek, N. Hogg, B. Kalyanaraman, Reaction of tetrahydrobiopterin with superoxide: EPR-kinetic analysis and characterization of the pteridine radical, Free Radic. Biol. Med. 31 (2001) 975–985.
[30] J. Vasquez-Vivar, Tetrahydrobiopterin, superoxide, and vascular dysfunction, Free Radic. Biol. Med. 47 (2009) 1108–1119.
[31] M. Delgado-Esteban, A. Almeida, J.M. Medina, Tetrahydrobiopterin deficiency increases neuronal vulnerability to hypoxia, J. Neurochem. 82 (2002) 1148–1159.
[32] L.J. Martin, N.A. Adams, Y. Pan, A. Price, M. Wong, The mitochondrial permeability transition pore regulates nitric oxide-mediated apoptosis of neurons induced by target deprivation, J. Neurosci. 31 (2011) 359–370.
[33] Q. Wang, L. Li, C.Y. Li, Z. Pei, M. Zhou, N. Li, SIRT3 protects cells from hypoxia via PGC-1alpha- and MnSOD-dependent pathways, Neuroscience 286 (2015) 109–121.